Towards Understanding Tear Progression of High-Grade Bursal-Sided Rotator Cuff Tendon Tears with Full-Field Strains

Carla Nathaly Villacís Núñez[1], Ulrich Scheven[1], Asheesh Bedi[2], Ellen M. Arruda[1]
[1]University of Michigan, Ann Arbor, MI, [2]NorthShore Orthopedic and Spine Institute, Chicago, IL
carlanvn@umich.edu

Disclosures: Carla Nathaly Villacís Núñez (N), Ulrich Scheven (N), Asheesh Bedi (1-Arthrex, 3B-Arthrex, 9-AOSSM Board), Ellen M. Arruda (N)

Introduction: Partial-thickness rotator cuff tendon tears can cause aggravating pain and disability, affecting between 13% and 32% of the general population, and 40% of overhead athletes. Both surgical and non-surgical treatments exist for high-grade (type III, >50% of footprint detachment) partial-thickness tears. However, determining when to operate is still a controversial topic, given that the natural history of these tears remains unclear, and tear evolution cannot be predicted based on the original characteristics of the tear. Biomechanical studies have utilized maximum strain concentrations in tear edges as a measure to determine full-thickness tear propagation directions. In most of these studies, surface strain is obtained, leaving aside the three-dimensional nature of the rotator cuff tendons and its effect on strain patterns and tear growth. Moreover, the leading edges of the tears are not visible in partial-thickness tears, which prevents their study from being performed using these in-plane strain measurement methods. Hence, our goal was to assess full-field strain changes between intact and partially torn rotator cuff tendons to elucidate tear progression mechanisms. Based on the Lagrangian shear strain maps our previous studies in type I and II partial-thickness tears showed, we hypothesized that delamination (mode II failure) would be a potential tear growth inducing mechanism in type III tears.
Methods: The infraspinatus tendon with its humeral attachment was isolated from five fresh ovine shoulders (footprint 9-14 mm). The bony attachment was shaped into a truncated pyramid for gripping purposes. Samples were mounted at neutral position (~0 degrees abduction/rotation) into 3D printed fixtures and inserted into a magnetic resonance imaging (MRI)-compatible apparatus (Figure 1-a and 1-b). Then, samples underwent cyclic uniaxial tension in the main direction of fibers inside a 7T small animal MRI coil. A displacement encoding protocol, called alternating pulsed gradient stimulated echo imaging (APGSTEi), was applied synchronously with the load-unload cycles to capture through thickness phase variation between deformed and undeformed configurations. Full-field displacements, Lagrange strains and maximum shear strains were calculated based on phase differences. Two clinically relevant configurations were tested in each sample, i) intact tendon, followed by ii) ~75% bursal footprint detachment (type III tear, ~75% thickness and ~75% width) with inverted U shape, created with a #10 scalpel blade (Figure 1-c). Two physiologically relevant displacements were analyzed for each condition, 1 mm and 2 mm (which were meant to represent submaximal and maximum human shoulder force ranges), for a total of four experiments per tendon. Binary masks were created with a custom-developed MATLAB (version 2023a) code to enclose regions of interest and calculate the percentage of change between intact and torn configurations. Masks were transformed into smooth meshes and displacements were interpolated to match these meshes.
Results: Complex displacement fields in all directions were registered for both intact and torn tendons (Figure 2-a and 2-b). The detached band of fibers in the torn configuration presented increased displacements along the pull direction as compared to its intact counterpart (Figure 2-b). Particularly, an increase of more than 4x was observed close to the detached bursal surface. A similar behavior was observed in the remaining attached portion of the fibers in the torn condition, with increases higher than 1.5x with respect to the intact configuration. In the torn tendons, non-uniform longitudinal and transverse displacements between the detached band of fibers and the remaining portion of fibers (Figure 2-b) produced shear strain magnitudes which surpassed 0.10 and 0.05 in the 1-2 and 2-3 directions, respectively (Figure 3-a and 3-b). This represented a variation of more than 0.10 in strain magnitude, in both components, with respect to the intact tendons. Maximum shear strains were concentrated in the region next to the detached surface, the articular surface, or the mid-substance (Figure 3-c), going beyond 0.08 close to the enthesis, which differed by more than 0.05 in magnitude when measured against the intact condition. For torn tendons with lower degree of tendon wrapping around the humeral head, larger displacements were registered in the region detached with the scalpel blade, as compared to the tendons with higher degree of wrapping. These values are reported for the 2 mm cyclic displacements and all tendons, and corresponding results for the 1 mm cyclic displacement followed a similar trend.
Discussion: As observed in our complex displacement maps, this animal model of the rotator cuff is a heterogeneous material whose three-dimensional structure cannot be disregarded. A high-grade partial-thickness tear in the bursal surface of the tendon produces significant changes in the longitudinal displacements and shear strains, with the detached band of tissue sliding on top of the still attached region. This behavior appears in composite materials with one family of fibers and has been visualized in transverse tears in tendons, encouraging the analysis of tendon tear progression via fiber-matrix debonding or matrix failure. Maximum shear strain variation of 0.05 represents more than 60% increase in the region close to the enthesis in the articular surface, which suggests that this area could be prone to tear progression even at a neutral position when using high shoulder forces. These results support our hypothesis that delamination could be a potential tear growth inducing mechanism in type III tears in the bursal surface. However, the threshold at which tear growth would occur has not been yet defined and we cannot ascertain if tear progression will occur. Our future work includes the characterization of fiber-matrix interactions to determine this threshold. Although our sample size is small, we observed fiber sliding and shear strains surpassing 0.10 in all tendons, so we would expect to see these trends in consecutive experiments with a larger sample size. Importantly, our animal model does not possess multiple fiber families or tendon load sharing as in the human rotator cuff tendons, but our technique could be applied to human cadaveric specimens and be combined with finite element models for the study of different partial-thickness and full-thickness tear types.
Clinical Relevance: We provide quantifiable evidence that high-grade partial-thickness tears in the bursal surface produce shear strains between the articular and bursal regions, which suggests that delamination could be a mechanism for tear progression. Successful measurement of shear strains and identification of damage thresholds in different tear types could inform when to perform repairs in tears at high risk of progression and the natural history of tears.

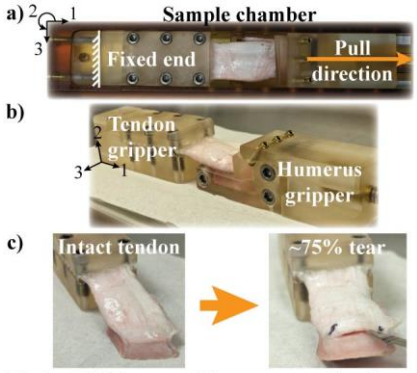

Fig 1. a) MRI compatible apparatus, showing loading direction. b) Fixture. c) Sample conditions.

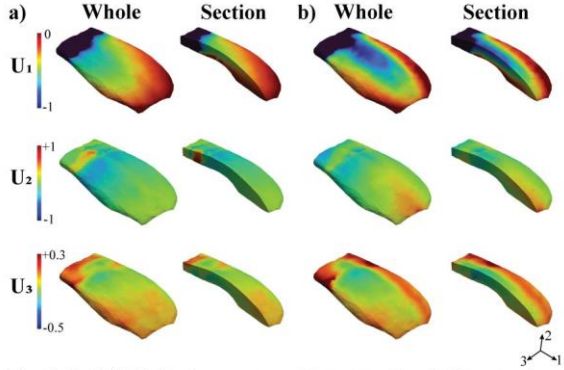

Fig. 2. Full-field displacements. a) Intact tendon, b) Torn tendon. 2 mm loading configuration is shown.

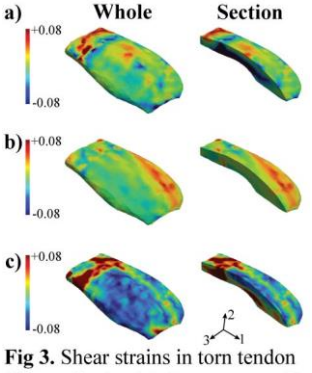

Fig 3. Shear strains in torn tendon (2 mm disp.). a) 1-2 component, b) 2-3 component, c) Maximum shear.